Neutron Reflectivity Study of Glassy Polymer Brushes in Density Fluctuating Supercritical Carbon Dioxide

TADANORI KOGA,[1] Y. JI,[1] Y. S. SEO,[2] C. GORDON,[3] F. QU,[3] M. H. RAFAILOVICH,[1] J. C. SOKOLOV,[1] S. K. SATIJA[2]

[1]Department of Materials Science and Engineering, State University of New York at Stony Brook, Stony Brook, New York 11794-2275

[2]Center for Neutron Research, National Institute of Standards and Technology, Gaithersburg, Maryland 20899

[3]Half Hollow Hills High School East, 50 Vanderbilt Parkway, Dix Hills, New York 11746

ABSTRACT: By using *in situ* neutron reflectivity, we measured the swelling behavior of two types of polymer brushes, deuterated polystyrene with a trichlorosilane end group and deuterated polystyrene-*block*-poly(4-vinylpyridine) block copolymer, in supercritical carbon dioxide (scCO$_2$). The measurements were conducted in the pressure range of 0.1–20 MPa at 36 °C. The pressure dependence of the brush height clearly showed an anomalous peak at the density fluctuation ridge (pressure = 8.2 MPa) that defined the maximum long-range density fluctuation amplitude in the pressure–temperature phase diagram of carbon dioxide (CO$_2$). The density profile of the brush, which could be approximated by a simple step function, and the magnitude of the brush height both indicated that the solvent quality of scCO$_2$ for the deuterated polystyrene brushes was still poor even at the density fluctuation ridge. In addition, atomic force microscopy images for the frozen polystyrene brush prepared by the rapid drying of CO$_2$ showed a phase-separated structure, as predicted from the numerical calculations of Grest and Murat, as a function of the variable $N\sigma$, where N is the polymerization index and σ is the grafting density. © 2004 Wiley Periodicals, Inc. J Polym Sci Part B: Polym Phys 42: 3282–3289, 2004
Keywords: neutron reflectivity; swelling; thin films

INTRODUCTION

Supercritical fluids (SCFs) have been widely used as regeneration solvents in a range of technical and chemical processes, such as chromatography, extraction, reactor cleanup, and the preparation of pharmaceutical products.[1] In addition, SCFs make ideal candidates for use in the development of new chemical processes because thermodynamic conditions can be used to control the solvating properties of these fluids. This thermodynamic control arises from the fact that the density of SCFs can be varied continuously from gaslike to liquidlike through modest changes in the pressure, temperature, or both. Density-dependent solvent properties, such as the solvent dielectric constant, diffusion coefficient, and viscosity, are thus also altered from gaslike to liquidlike values, and this causes corresponding changes in solute solvation. The greatest change in the solvent density is attained in the vicinity of the solvent's critical point, at which the solvent compressibility

is large, and small changes in the pressure yield large changes in the density. Although this hypersensitivity can be problematic, making process control difficult, there is still much interest in understanding and predicting solute solvation and reaction kinetics in the compressible regime around the critical point.

Near the critical point, solvent fluid molecules are apt to form large clusters, which induce *long-range density fluctuations*.[2] When solute molecules with an attractive solute–solvent interaction are dissolved in such fluids, the fluid solvent molecules rapidly attach to the solute molecules, and this results in density inhomogeneity. This process is often called *enhanced local density inhomogeneity* or *short-range density fluctuations* and exists only on a scale of a few angstroms.[3] Therefore, these two different length scales of solvent density inhomogeneities make SCFs scientifically interesting. Work over the past few decades has shown that the long-range density fluctuations influence the rate of increase in the solubility with respect to temperature and pressure, whereas the local density inhomogeneities control the absolute solubility.[4]

Much attention has been focused on supercritical carbon dioxide ($scCO_2$) because carbon dioxide (CO_2) has an easily accessible critical point (critical temperature = 31.3 °C and critical pressure = 7.38 MPa), is inexpensive, and is environmentally benign.[1] The major disadvantage of $scCO_2$ for polymer processing is that only a limited class of polymers, called CO_2-philic, such as highly fluorinated or silicone-based polymers, can be dissolved in CO_2 under relatively moderate conditions (<100 °C and <50 MPa). In many cases, either very high pressures or expensive CO_2-philic materials are needed. This places a severe restriction on the widespread use of $scCO_2$ as a solvent.

The large penetration depth inherent with neutrons makes neutron reflectivity (NR) an ideal tool for determining the *in situ* thickness, composition, and interfacial structure of polymer thin films immersed in fluids or gases under high pressure in thick-walled vessels. On the other hand, the technical difficulties involved in delivering the neutron beams into high-pressure vessels at glancing incidence have only recently been overcome by a new experimental chamber design.[5] Recently, we have found that a wide variety of polymer thin films can swell as much as 30–60% in CO_2 at the density fluctuation ridge, which defines the maximum long range density fluctua-

tion amplitude in CO_2, even when the bulk miscibility of the polymers with CO_2 is very poor.[6] Furthermore, the functional form of the swelling amplitude closely follows that of the calculated long-range density fluctuations as a function of the temperature and pressure. Hence, in contrast to previous ideas, the long-range density fluctuations directly control the absolute solubility of CO_2 in polymer thin films. In addition, we have found that anomalous swelling can be scaled with the polymer radius of gyration (R_g) and extended to a distance of approximately $10R_g$.[6]

The aim of this article is to study the swelling behavior at the density fluctuation ridge of the polymer brushes, the chain ends of which are chemically grafted to a solid surface. It is interesting to see whether this confinement of the chain ends leads to a different conformation than that of the free-chain situation in $scCO_2$. In addition, because polymer brushes can stretch without being removed from the substrate even in a good solvent, we can investigate the solvent quality of density fluctuating $scCO_2$ on the basis of the chain conformation perpendicular to the grafting surface.[7–14] For this study, we prepared two kinds of deuterated polystyrene (dPS) brushes on clean Si wafers: one was deuterated polystyrene with a trichlorosilane end group (dPS-$SiCl_3$), and the other was an asymmetric deuterated polystyrene-*block*-poly(4-vinylpyridine) block copolymer (dPS-*block*-P_4VP). Both the trichlorosilane ($SiCl_3$) and short poly(4-vinylpyridine) (P_4VP) end group bind to the Si surface. *In situ* NR measurements clearly showed that the pressure dependence of the swelling behavior for these two polymer brushes was the same as that of the non-tethered dPS thin film, including the anomalous swelling maximum at the ridge. Furthermore, the density profiles of the dPS brushes could be approximated by a simple step function within the entire pressure range used in this study, and this indicated that the solvent quality of $scCO_2$ was still poor even at the ridge.

We further studied the effect of $scCO_2$ exposure on the surface morphology of the polystyrene (PS) brush with atomic force microscopy (AFM). A hydrogenated polystyrene-*block*-poly(4-vinylpyridine) block copolymer (hPS-*block*-P_4VP) brush was first immersed in $scCO_2$ at the ridge and then quickly dried by flash evaporation of CO_2. As we have already reported,[15,16] this process vitrifies the polymer without the formation of micrometer-sized voids, which are known to form in the bulk when $scCO_2$ is forced under high pressures into

polymers with which it is immiscible.[17,18] The AFM results clearly showed a dimple structure of the brush within 1 nm of the air/polymer interface. Furthermore, for a carboxyl-terminated hydrogenated polystyrene (hPS) brush having the same grafting density (σ) as the PS-*block*-P$_4$VP brush, a similar dimpling structure occurred, but with an even larger roughness. This is consistent with a molecular dynamics (MD) simulation, which shows that the chain conformation of brushes in a poor solvent depends on σ as well as the polymerization index (N).[9]

EXPERIMENTAL

Materials

We prepared two kinds of polymer brushes for the NR experiments: one was a dPS-*block*-P$_4$VP block copolymer, in which P$_4$VP chains attractively adsorbed to the Si surface. The block copolymer consisted of 18 P$_4$VP units and 130 dPS units and was synthesized as previously described.[19] The brush was prepared via spin-coating onto a cleaned Si wafer. After the sample was rinsed in toluene, a good solvent for PS, a film thickness of 70 Å, corresponding to a σ value of 4.5×10^{-3} chains/Å^2, was obtained. The other brush was dPS [weight-average molecular weight (M_w) = 85,000] with an SiCl$_3$ end group, which offered a high binding energy ($\sim 10^2 kT$, where T is the absolute temperature and k is the Boltzmann constant) and allowed us to control σ by varying the reaction time and solution conditions.[10] To prepare the dPS-SiCl$_3$ brush, we exposed the clean Si crystal surface to a solution containing approximately 200 mg of polymer in approximately 100 mL of cyclohexane for 2 days at 4 °C. Unreacted polymers were washed off the surface by repeated exposure to toluene and dichloromethane, followed by an extended wash (~5 days) with toluene. The film thickness of the dry film was 140 Å, corresponding to a σ value of 1.1×10^{-3} chains/Å^2. To determine the effect of the chemically grafted chains on swelling, we also prepared a spin-cast thin film of non-tethered dPS without the end-terminated group [M_w = 690,000, weight-average molecular weight/number-average molecular weight (M_w/M_n) = 1.05; Polymer Laboratories].

For the AFM study, hPS (M_w = 380,000)-*block*-P$_4$VP (M_w = 37,000) was used. The film thickness of the dry brush sample was 190 Å after it was rinsed in toluene. The thickness of the brush was
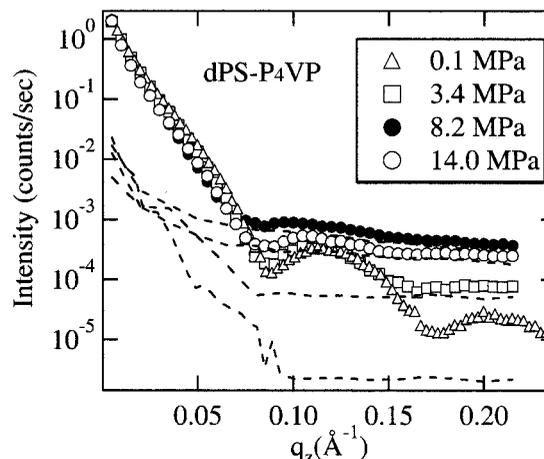

Figure 1. Raw reflectivity profiles for the dPS-*block*-P$_4$VP brush at 36 °C. The dotted lines show the background scattering from pure CO$_2$.

measured by ellipsometry. σ was estimated to be 3.0×10^{-4} chains/Å^2.

NR

Specular reflectivity measurements were performed on the NG7 neutron reflection spectrometer at the National Institute of Standards and Technology with a wavelength (λ) of 4.76 Å and a $\Delta\lambda/\lambda$ value of 2.5%. A high-pressure cell was designed and built by High Pressure Equipment Co. (Pennsylvania) specifically for these experiments.[5] The stabilities of the temperature and pressure of the cell were ± 0.1 °C and $\pm 0.2\%$, respectively. The exposure time before data collection was set to 1 h. The isothermal condition at 36 °C was maintained over pressures ranging from 0.1 to 20 MPa for both dPS brushes. The background scattering from pure CO$_2$ was also recorded simultaneously as a function of pressure because it is known to be a measure of the density fluctuations (see Fig. 1). After subtracting the background scattering intensity, we analyzed the data by comparing the observed reflectivities with calculated ones based on model density profiles with three fitting parameters—film thickness, scattering length density (SLD), and interfacial roughness between the polymer and CO$_2$—assuming a hyperbolic-tangent density function at the interface.[20] As discussed later, this simple step function could reasonably fit all the NR data, and this indicated that the solvent quality of CO$_2$ was poor for the dPS brushes.

AFM Experiments

The morphology of the brush structure for the PS-*block*-P$_4$VP brush was analyzed with a Digital Nanoscope III AFM instrument in the contact mode with an Si$_3$N$_4$ tip.

RESULTS AND DISCUSSION

Figure 2(a) shows representative NR profiles for the dPS-SiCl$_3$ brush at five different pressures and 36 °C; the reflected scattering intensity is plotted as a function of the momentum transfer normal to the surface, $q_z = 4\pi \sin \theta/\lambda$, where θ is the glancing angle of incidence and λ is the neutron wavelength. We obtained the data by successively increasing the pressure and then slowly decreasing the pressure. The results were identical, indicating that the swelling isotherm of the dPS-SiCl$_3$ brush was reversible. We can see that the film thickness, indicated by the frequency of Kiessig fringes, changed as a function of the CO$_2$ pressure. The solid lines are best fits to the data based on the single-layer profiles shown in Figure 2(b). Good fits were obtained with uniform concentrations of CO$_2$ in the polymer layer and no preferential adsorption of either CO$_2$ or polymer at the Si substrate. The height of the dPS-SiCl$_3$ brush changed from 140 Å at 0.1 MPa to 149 Å at 5.1 MPa, 161 Å at 8.2 MPa, and 153 Å at 10.3 MPa. Figure 3 shows the linear dilation (S_f) of the dPS-SiCl$_3$ brush, which was calculated with the equation $S_f = (L - L_0)/L_0$, where L and L_0 are the measured thicknesses of the swollen and unswollen polymer brushes, respectively. We can see a maximum of 0.15 in the S_f values at 36 °C and 8.2 MPa, which occurred at the density fluctuation ridge. Hence, it is clear that the anomalous swelling enhancement induced by the density fluctuations occurred regardless of the confinement of the chain ends. According to the NR measurements by Ivkov et al.,[21] the S_f value of the brush at the Θ condition, that is, in hydrogenated cyclohexane at 30 °C, was estimated to be 0.78. Therefore, we can say that the solvent quality of scCO$_2$ for the dPS brush was still poor even at the ridge. This was also confirmed by the fact that the simple step function provided a good model for all the data to represent the interface between the polymer and CO$_2$ layers, as shown in Figure 2(b). According to the numerical calculation with the self-consistent field lattice model,[22] the shape of the brush profile was a more boxlike shape in a poor solvent, whereas that in a good
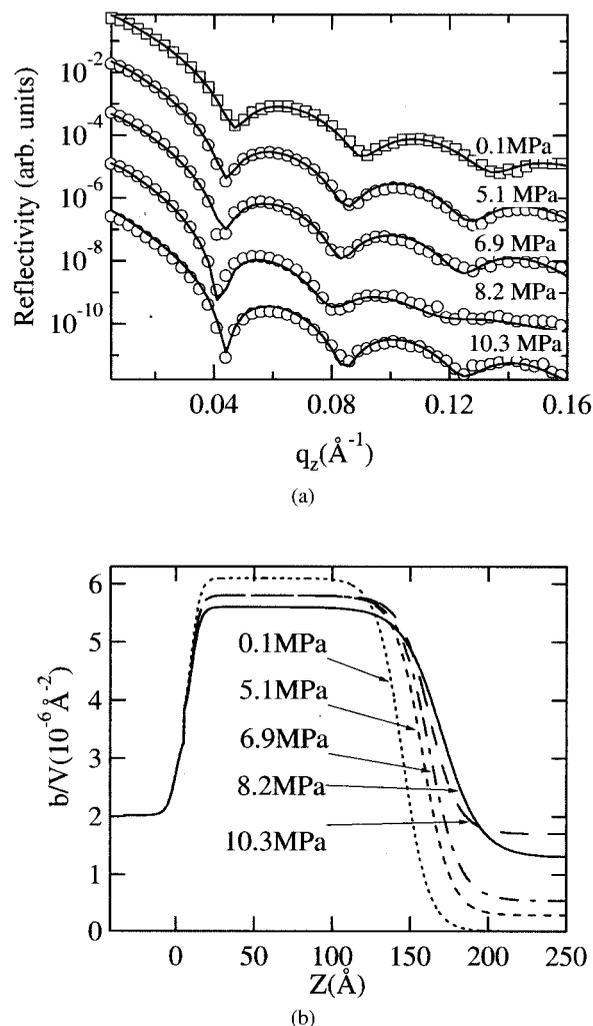

(a)

(b)

Figure 2. (a) Representative reflectivity data for the dPS-SiCl$_3$ brush at 36 °C. Consecutive reflectivities have been offset from one another for clarity. The solid lines represent reflectivities calculated from (b) the corresponding scattering length density (b/v) profiles as a function of depth (Z).

solvent was better approximated as a parabolic function.

To further compare the swelling behavior between the brush and non-tethered film, we also measured the NR curves for a dPS thin film without the end-terminated group at 36 °C. The thickness of the dPS film was larger than that of the brush film because we know from previous work that the magnitude of the S_f values is scaled with R_g.[5,23] Hence, the thicknesses chosen were such that the tethered and non-tethered films were approximately $2R_g$. The S_f values obtained from the NR spectra are also plotted in Figure 3 and are shown as filled circles. We can see no signifi-
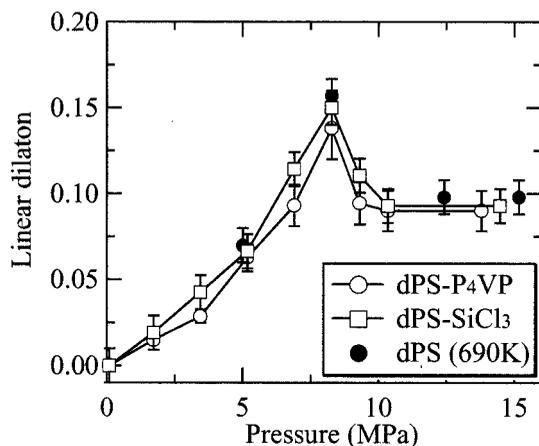
Figure 3. Pressure dependence of S_f at 36 °C.

cant difference in the swelling between the chemically end-grafted polymer and nongrafted polymer film in scCO$_2$. Furthermore, as we have reported, the concentration profiles of the non-tethered PS thin films were well fitted with the simple step function.[5,23] Hence, it seems reasonable to say that the chain conformation of the dPS film physically adsorbed to the Si substrate was equivalent to that of the brush in contact with scCO$_2$. In fact, our recent X-ray diffuse scattering data[24] indicate when the molecular weight of the polymer is higher than the entanglement length, the non-tethered PS films in air can be treated as adsorbed Guiselin brushes[25] with $N^{1/2}$ surface contacts.

Figure 4 summarizes the pressure dependence of the interfacial root-mean-square roughness (σ_{rms}) between the polymer and CO$_2$ layers for the both tethered and non-tethered dPS films. We can see that the *in situ* interfacial structures in CO$_2$ were also quantitatively equivalent to each other. In addition, we can see that both films showed sharp maxima at the ridge. Here the temperature was well below the glass-transition temperature of dPS (100 °C), and we were very sensitive to any changes in the segmental fluctuations. The abrupt increase in the interfacial roughness when S_f was large indicates that a drastic increase in the chain fluctuation time also occurred at the ridge. This is consistent with previous interdiffusion experiments for non-tethered dPS/hPS bilayers in CO$_2$, for which we found a sharp increase in the interdiffusion coefficient corresponding to an scCO$_2$-induced glass–liquid transition along the density fluctuation ridge.[15] Consequently, it seems quite reasonable that a similar density fluctuation-induced glass–liquid transition also occurs in dPS-SiCl$_3$ brushes.

As mentioned previously, the polymer chains are uniformly stretched away from the Si substrate in the poor scCO$_2$ solvent. Under poor solvent conditions, the thickness of the brush (h) follows the well-known scaling law:[7,26]

$$h \sim N\sigma \qquad (1)$$

To further explore this scaling argument in scCO$_2$, we measured the NR profiles for a dPS-*block*-P$_4$VP brush, the σ value of which was about four times higher than that of the dPS-SiCl$_3$ brush. The values for $N\sigma$ were 0.83 chains/Å^2 for the dPS-SiCl$_3$ brush and 0.58 chains/Å^2 for the dPS-*block*-P$_4$VP, and so a significant difference in the brush height was expected. The film thickness of the dry dPS-*block*-P$_4$VP brush was also approximately 2R_g. Figure 5 shows the representative reflectivity profiles of the dPS-*block*-P$_4$VP brush at 36 °C. The solid lines are fits to the single-layer profiles shown in Figure 5(b). As found for the dPS-SiCl$_3$ brush, a boxlike shape of the dPS-*block*-P$_4$VP brush was obtained from the fit. As shown in Figure 1, the q_z region was limited ($q_z < 0.16$ Å^{-1}) because of the high scattering intensity from CO$_2$, which prevented the quantitative determination of the interfacial roughness. The S_f values of the dPS-*block*-P$_4$VP brush are also plotted in Figure 3 and are shown by open circles. We can see that an anomalous maximum also occurred at 8.2 MPa in the dPS-*block*-P$_4$VP brush, and the entire swelling behavior was the same, regardless of the end grafting of the polymer thin films. Hence, it is clear that no significant effects of σ on the brush swelling were found in scCO$_2$. This is consistent with the fact that the
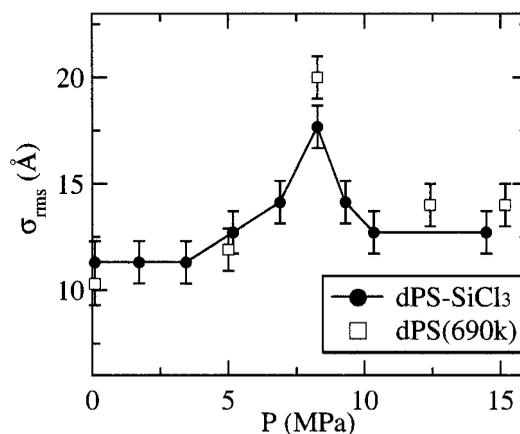

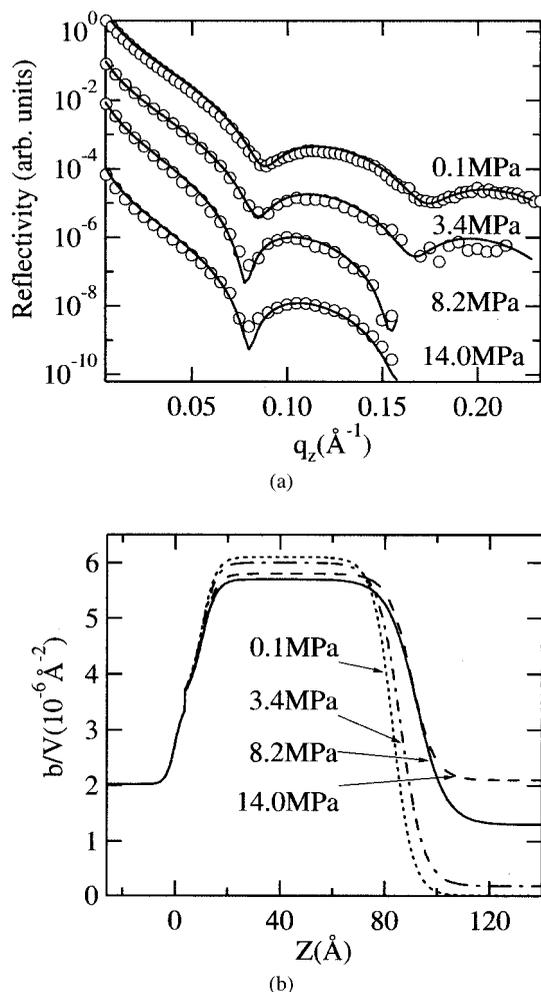**Figure 4.** Pressure dependence of σ_{rms} at 36 °C.

Figure 5. (a) Representative reflectivity data for the dPS-*block*-P$_4$VP brush at 36 °C. The solid lines represent reflectivities calculated from (b) the corresponding scattering length density profiles.

tethered chains have a near Gaussian conformation, which is similar to that of the non-tethered chains, which form Guiselin brushes. Thus, it may be appropriate to treat σ in eq 1 as a free parameter that can be arbitrarily fixed in the numerical calculation of the height of polymer brushes.

We now turn to the *ex situ* experiments for the PS(380,000)-*block*-P$_4$VP(37,000) block polymer brush with AFM measurements. The film thickness of the dry sample was prepared to be $1.2R_g$. Figure 6(a) shows AFM images (5 μm × 5 μm) of the PS-*block*-P$_4$VP brush before its exposure to scCO$_2$. On the left is a three-dimensional image, and on the right is a cross section along the line indicated in the left image. From these images,

we can see that a relatively homogeneous polymer brush was formed on the Si substrate. This was further confirmed by the AFM image analysis: the σ_{rms} value between the air and the polymer was only 5 Å. The brush was then exposed to scCO$_2$ under the ridge conditions, that is, 36 °C and 8.2 MPa. After the brush was immersed in scCO$_2$ for an annealing time of 3 h, we depressurized it to atmospheric pressure at a constant temperature within 10 s. As we previously reported for PS, this rapid sublimation of the gas preserved the swollen structure of the films.[15] From the ellipsometry experiment, we found that S_f of the brush was much larger ($S_f = 0.35$) than that of the short dPS-*block*-P$_4$VP brush obtained from the NR experiments ($S_f = 0.15$). This could be related to the difference in the dry film thickness scaled by R_g, as demonstrated with the non-tethered PS films.[6] According to the NR experiments, the S_f value of the non-tethered dPS film with the same scaled thickness ($1.2R_g$) as that of the PS-*block*-P$_4$VP brush was reported to be 0.31.[6] We are currently studying the scaled thickness dependence of the brush swelling along the ridge with a special rubbery polymer that enables us to prepare the dry film thickness up to about $8R_g$. The details will be reported elsewhere.

Figure 6(b) shows the AFM images for the PS-*block*-P$_4$VP brush after quenching. We can clearly see that lateral structures grew within 1 nm of the polymer/air interface. The average characteristic length of the lateral structures was estimated to be approximately 400 nm. Similar dimple structures of end-grafted polymer brushes have already been reported from theoretical[8,9,27] and experimental[28,29] studies to be a result of phase separation between polymer-rich and polymer-poor regions in the poor solvent regime. To determine whether the dimple structures observed also took place because of the poor solvent quality of CO$_2$, we made sure that the experimental parameters fell in an (N,σ) range[29] that allowed us to compare our results with the MD simulation reported by Grest and Murat.[9] Here we define a dimensionless scaling parameter (x) by comparing the typical dimensions of a polymer chain in a poor solvent with the average distance between the grafted point ($\sigma^{-1/2}$), that is, $x = N^{1/3}\sigma^{1/2}$. According to the MD simulation, the phase separation occurs in the low x regime ranging from 0.6 to 1.8, whereas a single homogeneous phase forms in the regime of higher values of x. For our experimental situation, the segment length of PS chain (a) was 6.7 Å, and σ of the
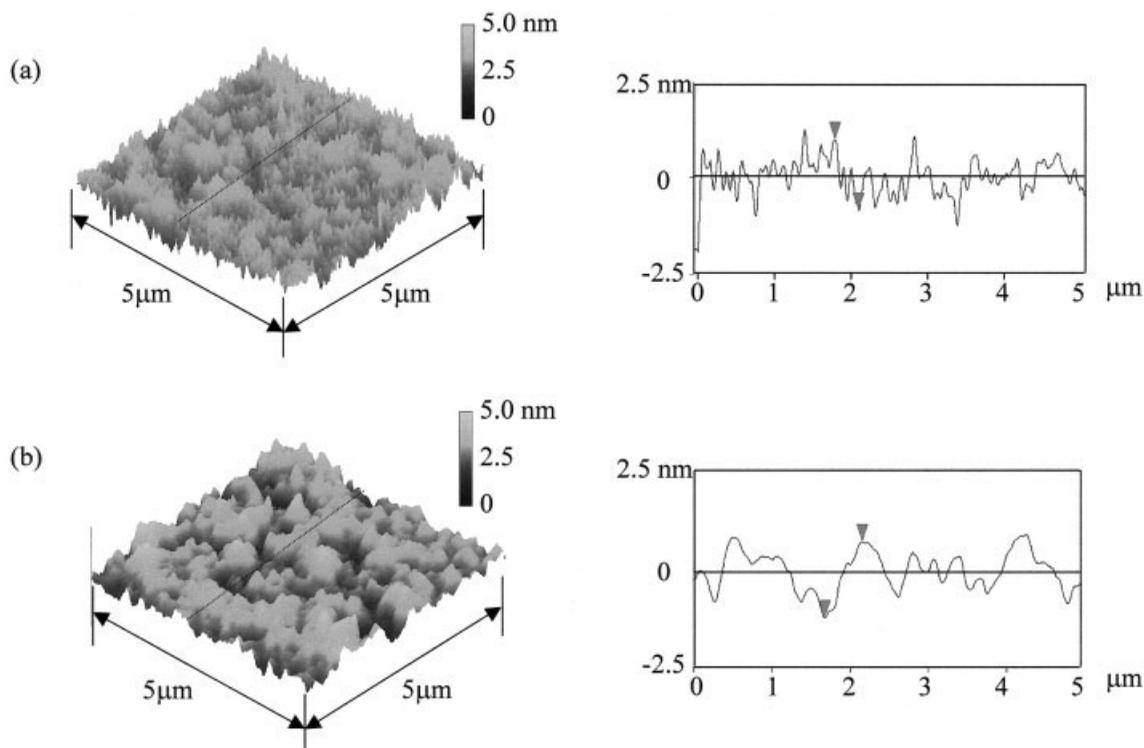
Figure 6. AFM images of the PS(380,000)-*block*-P$_4$VP(37,000) brush: (a) before exposure to CO$_2$ and (b) after exposure to CO$_2$ at 36 °C and 8.2 MPa and quick quenching.

brush was estimated to be 3×10^{-4} chains/Å^2. Accordingly, an experimental density of 0.013 grafting points in an area of 45 Å^2 was approximated. Consequently, substituting an experimental N value of 3653, we find an experimental x value (x_{exp}) of 1.75 for our systems, which is in good agreement with the values predicted for a poor solvent. To further explore the dimple structures, we prepared a carboxyl-terminated hPS brush ($N = 480$) with the σ value of 3×10^{-4} chains/Å^2. The x value for the carboxyl-terminated hPS brush was hence much lower ($x_{exp} = 0.9$). AFM images showed a similar dimpling structure after exposure to scCO$_2$, but with an even larger roughness (the data are not shown here). This is also consistent with the scaling of the x parameter in ref. 9. In contrast, no dimpling was observed with the homopolymer films. The dimpling would manifest itself only as a roughness of the total layer and hence could not be observed in the specular scattering of the NR data. On the other hand, it is a clear signature of the brush behavior of the tethered films. Therefore, we conclude that the phase separation observed in the hPS-*block*-P$_4$VP brush was induced by the poor solvent quality.

CONCLUSIONS

Using *in situ* NR, we measured the swelling behavior in scCO$_2$ of two polymer brushes, an end-functionalized dPS brush and a dPS-*block*-P$_4$VP block copolymer brush, the σ values of which differed by a factor of about 4. We found that along the density fluctuation ridge, anomalous swelling occurred with a maximum of $S_f = 0.15$ for both brushes, regardless of σ. This value was similar to that observed for a non-tethered homopolymer films of the same thickness scaled with R_g and was considerably smaller than that under the Θ condition ($S_f = 0.78$) measured by Ivkov et al.[21] The density profiles for all the films were well approximated by simple step functions, and hence we conclude that the solvent quality of scCO$_2$ for PS was still poor even at the density fluctuation ridge. AFM images of the films after the flash evaporation of scCO$_2$ revealed the formation of dimple structures of the hPS-*block*-P$_4$VP brush within 1 nm of the polymer/air interface. Similar structures were also observed for the carboxyl-terminated hPS brushes, for which the phase separation took place over the entire layer. This phase separation occurs only in polymer brushes,

and its amplitude is a function of σ and N, as observed.

REFERENCES AND NOTES

1. McHugh, M. A.; Krukonis, V. Supercritical Fluids: Extraction Principles and Practice; Butterworths: Woburn, MA, 1994.

2. Stanley, H. E. Introduction to Phase Transition and Critical Phenomena; Oxford University Press: Oxford, 1971.

3. Kajimoto, O. Chem Rev 1999, 99, 355–389.

4. Eckert, C. A.; Kuntson, B. L.; Debenedetti, P. G. Nature 1996, 383, 313–318.

5. Koga, T.; Seo, Y. S.; Shin, K.; Zhang, Y.; Rafailovich, M.; Sokolov, J.; Chu, B.; Peiffer, D.; Satija, S. K. Macromolecules 2003, 36, 5236–5243.

6. Koga, T.; Seo, Y. S.; Zhang, Y.; Shin, K.; Kusano, K.; Rafailovich, M. H.; Sokolov, J. C.; Chu, B.; Peiffer, D.; Occhiogrosso, R.; Satija, S. K. Phys Rev Lett 2002, 89, 125506-1-4.

7. Zhulina, E. B.; Borisov, V. A.; Birshtein, T. M. Macromolecules 1991, 24, 140–149.

8. Lai, P. Y.; Binder, K. J Chem Phys 1992, 97, 586–595.

9. Grest, G. S.; Murat, M. Macromolecules 1993, 26, 3108–3117.

10. Karim, A.; Satija, S. K.; Douglas, J. F.; Ankner, J. F.; Fetters, L. J. Phys Rev Lett 1994, 73, 3407–3410.

11. Perahia, D.; Wiesler, D. G.; Satija, S. K.; Fetters, L. J.; Sinha, S. K.; Milner, S. T. Phys Rev Lett 1994, 72, 100–103.

12. Kent, M. S.; Lee, L. T.; Factor, B. J.; Rondelez, F.; Smith, G. S. J Chem Phys 1995, 103, 2320–2342.

13. Satija, S. K.; Gallagher, P. D.; Karim, A.; Fetters, L. J Phys B 1998, 248, 204–207.

14. Karim, A.; Tsukruk, V. V.; Douglas, J. F.; Satija, S. K.; Fetters, L. J.; Reneker, D. H.; Foster, M. D. J Phys II 1995, 5, 1441–1456.

15. Koga, T.; Seo, Y. S.; Hu, X.; Kwanwoo, S.; Zhang, Y.; Rafailovich, M. H.; Sokolov, J. C.; Chu, B.; Satija, S. K. Europhys Lett 2002, 60, 559–565.

16. Koga, T.; Jerome, J.; Seo, Y. S.; Ge, S.; Seeck, O. H.; Rafailovich, M. H.; Sokolov, J. C.; Tolan, M.; Kolb, R.; Chu, B. Appl Phys Lett 2003, 83, 4309–4311.

17. Stafford, C. M.; Russell, T. P.; McCarthy, T. J. Macromolecules 1999, 32, 7610–7616.

18. Arora, K. A.; Lesser, A. J.; McCarthy, T. J. Macromolecules 1998, 31, 4614–4620.

19. Gauthier, S.; Eisenberg, A. Macromolecules 1987, 20, 760–767.

20. Russell, T. P. Mater Sci Rep 1990, 5, 171–271.

21. Ivkov, R.; Butler, P. D.; Satija, S. K.; Fetters, L. J. Langmuir 2001, 17, 2999–3005.

22. Wijmans, C. M.; Scheutjens, J. M.; Zhulina, E. B. Macromolecules 1992, 25, 2657–2665.

23. Koga, T.; Shin, K.; Zhang, Y.; Seo, Y. S.; Rafailovich, M. H.; Sokolov, J. C.; Chu, B.; Satija, S. K. J Phys Soc Jpn 2001, 70, 347–349.

24. Seo, Y.; Koga, T.; Sokolov, J.; Rafailovich, M. H.; Tolan, M.; Sinha, S. K.; Kolb, R. Phys Rev Lett, submitted for publication, 2004.

25. Guiselin, O. Europhys Lett 1992, 17, 225–230.

26. Halperin, A.; Tirrel, M.; Lodge, T. P. Adv Polym Sci 1991, 100, 31–71.

27. Yeung, C.; Balazs, A. C.; Jasnow, D. Macromolecules 1993, 26, 1914–1921.

28. O'Shea, S. J.; Welland, M. E.; Rayment, T. Langmuir 1993, 9, 1826–1835.

29. Zhao, W.; Krausch, G.; Rafailovich, M.; Sokolov, J. Macromolecules 1994, 27, 2933–2935.